Original Article

Insights on the structural characteristics of Vim-TBS (58-81) peptide for future applications as a cell penetrating peptide

Avneet Saini*, Radhika R. Jaswal, Riteshwari Negi, Fateh S. Nandel

Department of Biophysics, Panjab University, Chandigarh, India.

Summary   The plasma membrane presents a remarkable barrier for the delivery of peptide and nucleic acid based drugs to the inside of cells. This restraint in the path of their development as therapeutic agents can be offset by their conjugation to cell penetrating peptides (CPPs) that can lead to an improved pharmacological profile. In this context, conformational behavior of Vimentin Tubulin Binding Site (TBS) peptide, Vim-TBS (58-81), was investigated for its acknowledged cell penetrating properties along with Trans-activating Tat (48-60) peptide and a pro-apoptogenic peptide of p21/WAFI protein (p10). Also, the fusion peptides Vim-TBS (58-81)-p10 & Tat (48-60)-p10 were studied using molecular mechanics (MM) and molecular dynamics (MD) based strategies. MM results revealed formation of stable α-helix like secondary structures in Vim-TBS (58-81), Tat (48-60) and p10 peptides. In water, three peptides adopted either a helical structure or a random conformation; the stability of either of the two states being governed by the formation of polar contacts with the solvent. The fusion peptides formed helical structures after MD simulations but the structure obtained for the fusion peptide, Vim-TBS-p10 is relatively better characterized in terms of its amphipathic nature with a hydrophilic face formed by the positively charged residues facilitating a better interaction of this fusion peptide with the membrane as compared to that of Tat-p10 peptide. This is the first report on the conformational characteristics of the Vim-TBS (58-81) peptide and the fusion peptide, Vim-TBS (58-81)-p10. The results presented here are significant for their potential role in guiding and facilitating the future efforts of designing peptide based cell penetrating drugs.

Keywords: CPPs, Vim-TBS, Tat, p10, peptides, molecular mechanics, molecular dynamics

1. Introduction

Living cells are protected from their surrounding environment by cell membranes that only allow movement of small molecular size compounds across their barrier. During the last two decades, a number of peptides presenting the ability to be translocated across biological membranes have been identified and thoroughly studied, resulting in the characterization of a new family of peptides known as cell-penetrating peptides, in some cases also frequently referred to as protein transduction domains (PTDs) (*1*). CPPs are short (~35 amino acids) water soluble, partly hydrophobic or polybasic peptides that are capable of entering most mammalian cells at low molecular concentrations *in vivo* and *in vitro* without using any chiral receptors and without causing significant membrane damage (*2*). Many CPPs are highly cationic, usually rich in arginine and lysine amino acids and hydrophilic, exhibiting no or relatively low amphipathicity when compared to other peptides that are known to interact with and permeabilize phospholipid membranes. The mechanism of penetration of CPPs is ambiguous, but ample evidence prevails for multiple mechanisms, including direct translocation across the plasma membrane and endocytosis (*3*).

The profound interest that CPPs evoked among the scientific community was associated not only with their ability to cross cellular membranes by a non-toxic process, apparently independent of membrane receptors and energy consumption, but mainly due to the capacity

Address correspondence to:
Dr. Avneet Saini, Department of Biophysics, Panjab University, Chandigarh 160014, India.
E-mail: avneet@pu.ac.in

to promote the efficient cellular internalization of bio-molecules/drugs conjugated to these peptides (*4-11*). Since, the lack of permeability of the cellular membranes to hydrophilic bio-molecules constitutes one of the most important barriers to the delivery of therapeutic agents; this discovery has been regarded as an important step towards the development of novel strategies to increase the intracellular availability of molecules with high therapeutic interest but with low membrane permeability. Furthermore, CPPs are capable of carrying cargoes of a wide range of molecular size such as proteins (*12,13*), oligonucleotides (*14*) and even 200 nm liposomes (*15,16*) into different cellular compartments. Therefore, they are extremely attractive candidates to transport drugs to the interior of the cell. These peptides are also of profound interest in imaging processes, specifically in case of cancerous cells (*17*). The penetration of CPPs into cells is usually rapid and of first-order, with half-times from 5 to 20 minutes (*18*).

Among all CPPs, which include protein transduction domains (*19*), chimeric peptides and peptides of synthetic origin, the peptides derived from the HIV-1 Tat protein (*1*), from the homeodomain of the Antennapedia protein of Drosophila (Tat and Penetratin peptides, respectively), as well as the synthetic Pep-1 peptide (*20*), are the best characterized. These peptides have been successfully used for the intracellular delivery of different cargoes (*21*), including nanoparticles, full-length proteins, liposomes and nucleic acids, both *in vitro* and *in vivo*, thus resulting in successful transduction in animal tissues, including the brain.

Intermediate filaments (IFs) by binding to unpolymerized tubulin at discrete tubulin binding sites, provides flexible intracellular scaffolding which imparts structure to cytoskeleton hence, providing resistance to the cell from external stresses (*22*). In a recent report, a peptide Vim-TBS 58-81 corresponding to the tubulin binding site of the type III IF protein Vimentin, has been shown to enter cells (*23*) using well-established cell biology techniques (*24*). Furthermore, the inhibition of cell proliferation through nucleus localization of Vim-TBS 58-81 coupled to p10 (a pro-apoptogenic peptide of p21/WAFI protein, an established model peptide to evaluate the translocation efficiency of CPPs) has been reported (*25*).

To the best of our knowledge, no work has been done on the conformational characterization of the vimentin-tubulin binding site peptide, Vim-TBS (58-81), for its cell penetrating properties. Therefore, the primary aim of this project is to evaluate its conformational preferences in terms of various interactions that tend to guide and stabilize its structure. To have an in depth knowledge of its structural characteristics, structural properties of Tat (48-60) and p10 peptides were also studied. Tat (48-60) and p10 were particularly selected as the former is a well studied CPP and the later is a pro-apoptogenic fragment of p21/WAFI protein that is often used as a model cargo to evaluate cell penetrating properties. As structural versatility has been described as an important factor to be considered for deciphering cellular uptake properties by CPPs (*26-28*) the present work supports the hypothesis that structural plasticity could have a crucial role on its properties and functionality. Therefore, we examined the conformational aspects in a step by step approach that begins by the identification of intrinsic properties of the peptides through refined systematic fragmentation as shown in Table 1 and 2. The structural states and conformational plasticity of peptides in distinct environmental models was studied using molecular mechanics and molecular dynamics approaches. Finally, conformational preferences of the fusion peptides Vim-TBS (58-81)-p10 and Tat (48-60)-p10 were analyzed by MD simulations in explicit water as solvent.

Table 1. Amino acid sequence of different peptides investigated

Peptide	Sequence
Tat 48-60	GRKKRRQRRRPPQ
Vim-TBS 58-81	GGAYVTRSSAVRLRSSVPGVRLLQ
p10	RQTSMTDFYHSKRRLIFS
Vim-TBS 58-81-p10	GGAYVTRSSAVRLRSSVPGVRLLQ-RQTSMTDFYHSKRRLIFS
Tat 48-60-p10	GRKKRRQRRRPPQ -RQTSMTDFYHSKRRLIFS

Table 2. Model oligopeptide fragments of Tat (48- 60), Vim-TBS (58-81), p10 peptides

Tat. (48- 60) peptide				Vim-TBS (58-81) peptide					p10 peptide			
I	II	III	IV	I	II	III	IV	V	I	II	III	IV
G^{48}	K^{51}	Q^{54}	R^{57}	G^{58}	V^{62}	A^{67}	S^{73}	V^{77}	R^1	M^5	Y^9	K^{12}
R	R	R	P	G	T	V	V	R	Q	T	H	R
K	R	R	P	A	R	R	P	L	T	D	S	R
K	Q	R	Q	Y	S	L	G	L	S	F	K	L
R^{52}	R^{55}	P^{58}	Q^{60}	V	S	R	V	Q^{81}	M	Y	R	I
				T	A	S	R^{78}		T^6	H	R^{14}	F
				R^{64}	V^{68}	S				S^{11}		S^{18}
						V^{74}						

2. Methods

To gain insights on the Φ, Ψ, ω, & χ values and thus, on the potential energy space explored by each amino acid residue, the peptide sequences were divided into short overlapping model oligopeptide fragments, each containing five to seven amino acid residues (Table 2). Understanding secondary structure of peptides is a prerequisite for functional characterization. Since, most of the peptide secondary and tertiary structures are not available in Protein Data Bank (PDB) secondary structure prediction methods are used to obtain crucial knowledge about the structure and function of the peptides. PSIPRED, a web server (*29*) based on such prediction methods, was used to gain valuable insights into the type of secondary structure these peptides may possibly adopt. These prediction results (results not shown) provided the initial background on the various possible starting conformations for energy minimization studies. Hence, different starting conformations were taken along with a linear starting geometry. Every oligopeptide fragment was then minimized by MM based software- Swiss pdb Viewer (*30*), using a steepest descent and conjugate gradient method with a cut-off of 0.05 kJ/mol. MM energy minimization calculations were then performed on the full length peptides *i.e.* Vim-TBS (58-81), Tat (48-60) and p10 at a dielectric constant of 4, using different starting conformations based on the minimization results of model oligopeptides together with the conformations obtained from the secondary structure prediction results. The results thus obtained were analyzed in terms of the various stabilizing interactions.

Simulations provide a great deal of information with respect to the stability of non-covalent interactions in water and gain insight on the dynamic characteristics of the peptides in solvent. GROMACS software was used for the MD studies (*31*). Interaction parameters for the simulations were taken from GROMOS-96 force field (*31*). Energy of the system was minimized with the convergence value (emtol) of 1000 kJ mol^{-1} nm^{-1}. In order to allow equilibration of solvent around the model sequence, the position of all residues was restrained for 20ps at the desired temperature. MD simulations were performed for 1ns in an NVT ensemble with water (*32*) as solvent at a constant temperature of 300K *i.e.* at constant volume, temperature, and mass. The run was carried out with a time step of 2fs using the Leap Frog Algorithm (*33*) and temperature was controlled through weak coupling to a constant temperature bath (*34*) using a coupling time constant; τ_p of 0.1ps and a reference temperature; T_0 of 300, 313 & 343 K. LINCS algorithm (*35*) was used to restrict all bonds to their equilibrium lengths and the center of mass motion of the system was removed at every step to maintain the effective simulation temperature at 300 K. Pressure was controlled using weak coupling with a time constant of 0.5 ps and a reference pressure of 1 Bar. For the

evaluation of coulomb interactions and Van der Waals interaction a cut off of 0.9 and 1.0 nm respectively was applied. Long range forces were updated every 10fs during generation of the neighbor list. Long Range Electrostatic Interactions were calculated using a Particle Mesh Ewald Summation (*36*). Initial velocities of all atoms were taken from a Maxwellian distribution at the desired initial temperature. Because we aim to establish the conformational characteristics of vimentin tubulin binding peptide for its potent applications as a cell penetrating peptide, MD simulations of this peptide in conjunction with p10 (fusion peptide) were also carried out along with the simulations of the fusion peptide Tat 48-60-p10 (acting as control for the study) at 300 K with the same MD parameters (*31*) for 1 ns under NVT conditions. The results obtained were analyzed using VMD software (*37*). Detailed analysis will help in the understanding of the interactions playing key roles in the mechanism of cell penetration. All simulations were carried out using the GROMACS Molecular Dynamics Package on the Desktop FUJITSU Workstation R570-2.

3. Results

3.1. *MM energy minimizations*

3.1.1. *Model oligopeptides*

In order to best explore the potential energy surface, three different starting geometries were taken (based on the PSIPRED Prediction results) for minimization of the various model oligopeptides of Vim-TBS 58-81 with Φ, Ψ values of -57°, -47°; -139°, 135° & 180°, 180° corresponding to α-helix, β-strand and linear conformations respectively. This preference of Φ, Ψ values is also based on extensive study of previous work on usual and unusual peptides/peptoids (*38-40*). On the basis of energy, the most stable conformations obtained after steepest descent minimization followed by a conjugate gradient method for various model oligopeptides of Vim-TBS 58-81, Tat 48-60 and p10 peptides are discussed in Table 3. It is evident from the results that the most stable conformation in all model oligopeptides of Vim-TBS (58-81) populated the second quadrant of the Ramachandran map with Φ, Ψ values of ~ -100°, 110° (± 30°) except for model oligopeptide IV. Such structures are particularly stabilized by minimization of steric constraints imposed by the lengthy and/or bulky aromatic and/or charged side chains. Also, CH⋯π interactions and hydrophobic interactions lend stability to such conformations. In model oligopeptide IV no regular secondary structure was observed as large deviations in the Φ, Ψ values of particularly the centrally placed proline and glycine residues were observed. Proline is a known and most efficient helix breaking residue in natural proteins and peptides because its nitrogen cannot form hydrogen bonds (*41*). On the other

hand, glycine is the simplest least restricted amino acid and thus, can explore a larger conformational region favoring a larger number of possible combinations of Φ, Ψ values on the Ramachandran map (*42,43*). Therefore, the consecutively positioned proline and glycine residues (with contrasting conformational behavior) are argued to be responsible for the non-regular/random secondary structure in oligopeptide IV.

The peptide Tat (48-60) is highly positively charged and is predicted by PSIPRED to adopt a helical structure (except residues 57-60 that are predicted to adopt a coil like structure). Keeping these observations

Table 3. Molecular mechanics results for the most stable conformational states of various model oligopeptides

Vim-TBS 58-81

Fragment I	G	G	A	Y	V	T	R	
Φ	-	-175.4	-119.4	-126.0	-76.4	-68.6	-118.6	
Ψ	146.6	152.7	148.8	143.0	88.1	86.3	-	
ω	-	-178.3	-177.9	-171.2	178.1	-177.7	175.2	
Fragment II	V	T	R	S	S	A	Y	V
Φ	-	-69.6	-115.0	-117.1	-114.5	-115.1	-116.9	-116.2
Ψ	139.7	87.4	99.6	148.3	149.2	138.9	-	-
ω	-	177.4	-178.0	179.6	178.8	178.9	-178.3	-179.4
Fragment III	A	V	R	L	R	S	S	
Φ	-	-76.5	-68.8	-71.4	-123.0	-116.7	-110.4	
Ψ	143.2	88.4	85.2	81.3	145.1	149.3	143.8	
ω	-	178.3	-179.4	175.5	-175.3	179.4	178.8	
Fragment IV	S	V	P	G	V	R		
Φ	-	-103.9	-60.5	62.8	-130.4	-111.6		
Ψ	96.2	126.4	132.5	-148.5	82.8	-		
ω	-	-175.9	176.2		179.0	-179.8		
Fragment V	V	R	L	L	Q			
Φ	-	-70.6	-69.0	-74.3	-120.2			
Ψ	103.1	86.4	81.3	77.4	-			
ω	-	177.8	177.4	178.0	-175.8			

Tat 48-60

Fragment I	G	R	K	K	R
Φ	-	55.6	-63.2	-81.1	-127.9
Ψ	-152.6	-95.5	35.7	39.9	-
ω	-	-178.5	172.7	-179.7	-179.1
Fragment II	K	R	R	Q	R
Φ	-	-50.8	-57.4	-90.3	-72.5
Ψ	-91.1	-47.8	-26.3	-32.2	-
ω	-	-176.2	178.2	179.7	-174.1
Fragment III	Q	R	R	R	P
Φ	-	-73.4	-79.2	-114.0	-57.3
Ψ	-154.3	72.6	81.8	106.0	-
ω	-	172.6	176.5	-173.6	178.2
Fragment IV	R	P	P	Q	
Φ	-	-48.1	-58.6	-66.6	
Ψ	-39.8	-32.2	-29.8	-	
ω	-	-179.9	170.2	-177.3	

P10

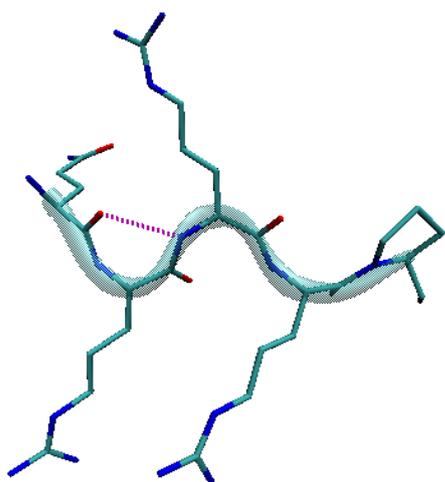| Fragment I	R	Q	T	S	M	T	
Φ	-	49.9	-59.5	-64.1	-70.5	-68.7	
Ψ	-28.6	-45.6	-55.9	-28.7	-44.3	-	S
ω	-	176.5	178.0	176.5	171.4	-175.4	-65.4
Fragment II	M	T	D	F	Y	H	-
Φ	-	-55.5	-50.4	-64.8	-61.5	-69.7	178.1
Ψ	-32.2	42.1	-41.4	-46.6	-35.7	-42.7	
ω	-	-177.9	176.1	177.7	175.6	175.1	
Fragment III	Y	H	S	K	R	R	S
Φ	-	-58.0	-59.7	-58.0	-65.4	-70.8	-63.3
Ψ	-29.3	-40.5	-46.0	-35.3	-29.5	-	-
ω	-	-177.8	172.6	177.4	176.9	172.0	178.8
Fragment IV	K	R	R	L	I	F	
Φ	-	-47.0	56.2	-64.8	-60.1	-64.6	
Ψ	146.6	-50.1	-39.5	-45.3	-42.5	-42.6	
ω	-	178.5	175.3	176.5	175.2	175.3	

Figure 1. Characteristic 2_7 ribbon structure is observed in Vim-TBS model oligopeptide III, where arginine residues are placed consecutively.

in consideration along with the properties and functionalities of the consecutively placed residues, various model oligopeptides were designed in such a manner that each fragment was not more than 5 residues in length. As it is clear from the results in Table 3, these model oligopeptides showed variable conformations contrary to the prediction results for the peptide thus signifying the importance of length and nature of the amino acid residues. A careful and critical analysis of these results particularly in the case of model oligopeptides I & III revealed that whenever lysine and arginine are placed consecutively (model oligopeptide I) no uniform structure is formed, while a uniform helical structure was observed when only arginine residues were positioned consecutively (model oligopeptide III), as apparent from the graphical view in Figure 1. This can be explained on the basis of formation of seven membered hydrogen bonds between the carbonyl-oxygen of the ith residue and amide hydrogen of the $i^{th}+2$ residue *i.e.* Arg $d_{COi..HNith+2}$ = 2.03, 2.27 Å and carbonyl-carbonyl interactions resulting in the formation of the 2_7 ribbon structure (Figure 1) (*44*). Thus, it would not be wrong to say that the type of positively charged residue plays a crucial role in designing a helical secondary structure of short length cationic oligopeptides like in the protamine family of cationic peptides (mainly composed of arginine 70%) (*45,46*). Further, a short model oligopeptide IV corresponding to residues 57-60 of Tat (48-60) (that were predicted to adopt a coiled structure) is designed specifically to contain two consecutively placed proline residues in the center. Contrary to the well known fact that proline facilitates formation of protein secondary structure elements such as turns and the polyproline II helix, but typically disfavors α-helix and β-strand conformations (*47*). It was observed that in this model oligopeptide both proline residues adopt Φ, Ψ values characteristic of 3_{10} helices and further results in the formation of a strong ten membered hydrogen bond

Table 4a. Molecular mechanics results for Vim-TBS (58-81) peptide

Seq ↓	State I	State II	State III
G	-,141.6 -	-,90.1 -	-,146.7 -
G	54.2,-107.8 178.6	-49.4,-37.7 -177.8	-175.4,153.6 -178.4
A	-55.9,-38.6 177.2	-51,-41.6 175.8	-118.6,146.8 -178.9
Y	-64.5,-29.1 176.4	-66.3,-38.7 -179.6	-112.2,94 -169.8
V	-64,-49 175.5	-59.8,-55.4 175.4	-70.6,89.6 -179.6
T	-73.9,16.7 -171.5	-58.6,-35.1 175.1	-69.2,83.7 178.4
R	125.3,142.7 -174.5	-62.2,-52.9 172.2	-73.7,85.7 179.3
S	-56.3,96 -174.5	-60.2,-41.8 178.1	-121,148.1 177.4
S	-153.1,-176.1 -171.9	-66.9,-38.8 175.2	-113.5,142.8 178.2
A	-72.5,74.8 179.5	-58.5,-43.5 169.5	-72.3,83.9 176.1
V	-123.6,137.7 178.1	-58.4,-45.2 -172.8	-72.5,81.5 177.4
R	-45.68,-38.8 -178.1	-57.9,-46.1 175	-72.5,82.1 -178
L	-44.4,-39.3 176.6	-57.9,-44.6 174.8	-73.1,78.9 175
R	-81.5,46 -179	-58.7,-60.5 174.6	-117.3,99 -175.2
S	-169.1,-157 178.8	-61.2,-29.5 -177.6	-115,144.4 179.3
S	-161.6,89.3 173.5	-54.1,-34.8 173.8	-119.1,148.2 179
V	-118.9,91.3 165.9	-68.7,-48.3 179.3	-113,103.9 177.3
P	-57.9,108.1 -171.1	-54.2,-39.6 165.7	-64.6,92.6 175.4
G	64.9,164.9 -7	-54.9,-50.4 172.2	-68.6,78.8 176
V	-122.6,89.2 170.3	-56.4,-47.6 174.1	-73.7,86.6 179.5
R	-121.3,160.9 179.2	-55.8,-45.6 176.3	-69.1,84.2 177.8
L	-40.1,-46.3 -176.6	-62.7,-38.4 175.6	-69.2,80.2 176.9
L	-104.7,29.5 -177.8	-66.7,-36.6 172.6	-74.2,77 177.6
Q	-125.5,- 176.7	-63.1,- 177.7	-119.3,- -175.7
ΔE kcal/mol	29.7	0.0	96.4

between the carbonyl oxygen of the first arginine residue and the amide hydrogen of the fourth amino acid residue, $d_{COi...HNi+3}$ = 1.86 Å. Energy minimization results of the various model oligopeptides of p10 revealed the formation of helical secondary structures stabilized by strong carbonyl...carbonyl interactions and a strong hydrogen bond network (Table 3).

3.1.2. *Full-length peptides*

Molecular mechanics energy minimization results of

Table 4b. Molecular mechanics results for different conformational states of Tat (48-60) peptide and p10 peptide

Tat (48-60) peptide			p10 peptide		
Seq.↓	I	II	Seq.↓	I	II
G	-,94.6 -	-,-149.3 -	R	-,-24.6 -	-,99.1 -
R	-62.2,-83.5 -175.7	49.7,-94 178.8	Q	-48.2,-43.3 -176.3	-123.5,146.1 179.8
K	-118,-3.9 171.3	-55.4,-41.1 176.1	T	-60.1,-64.5 176	-69.7,90.9 178.5
K	-99.9,119.9 -169.7	-58,-44.9 176.6	S	-56.9,-44.7 179.3	-67.8,84.4 175
R	-173.5,153.4 173.5	-64.7,-45.2 178.7	M	-60.7,-49.4 177.5	-72.6,85.7 -177.2
R	-49.8,-39.9 169.3	-58.7,-45.4 175.6	T	-63.8,-40.9 175	-70.1,23.3 -178.9
Q	-90.6,36 174.8	-58.7,-45.2 174.1	D	-55.7,-44.5 172	-84.9,34.7 -158.8
R	-171.4,-152.9 173.6	-60.3,-40 174.9	F	-58.6,-51.6 173.2	-88.6,39.9 -177.3
R	-81.9,91.6 -176.3	-63.2,-31 175.9	Y	-56,-47.4 177.5	-82.2,81.6 -174
R	-122,100.3 163.6	-59,-41.5 -175.2	H	-59.1,-46.2 174.3	-121.3,100 -172.2
P	-58.9,135.1 177	-62.8,-37.7 172	S	-61.4,-38.7 174.7	-70.4,82.1 176.7
P	-599,-41.7 174.9	-64.8,41.3 163.9	K	-61.3,-46.5 173.2	-69,80.9 179.6
Q	-75.8,- 173.1	-61.9,- 177.3	R	-57.2,-46.3 173.6	-72.6,76.5 178.6
			R	-58.1,-42.9 174.9	-73.4,79.4 -178.6
			L	-59.2,-45.8 173.1	-75.8,74.7 -179
			I	-59.6,-43.7 174.3	-78.1,88.7 -177.2
			F	-64.1,-36.7 176.9	-122.9,143.1 176.3
			S	-60.8,- -178.8	-113.9,- 179.8
ΔE kcal/mol	33	0.0	ΔE kcal/mol	0.0	61.8

the full length peptides *i.e.* Vim-TBS (58-81), Tat (48-60) and p10 are as summarized in Table 4a & b.

3.1.3. *Vim-TBS (58-81)*

Three different starting conformations were taken for minimization studies based on the prediction server results as well as the model oligopeptide minimization results. The first conformation called 'State I' corresponds to a state with starting geometry obtained after model oligopeptide fragment minimization calculations. The prediction server results have shown the propensity of both β-strand and coil type secondary structure throughout the sequence, and therefore Φ, Ψ values of the other two starting conformations correspond to β-strand *i.e.* -139°, 135° (State III) and α-helix *i.e.* -57°,-47° (State II). It is evident from the results in Table 4a that the energetically most stable conformation is State II with Φ, Ψ values of ~ -59.3°,-45.3° forming a characteristic α-helix like secondary
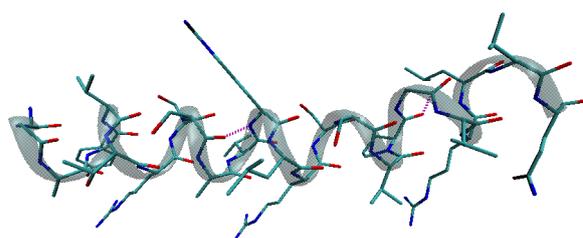

Figure 2. Intra-strand hydrogen bond network and carbonyl-carbonyl interactions stabilize Vim-TBS (58-81) peptide in the α-helical conformation.

structure. A molecular view of this conformation given in Figure 2 depicts the typical intra-strand hydrogen bonding network along with strong carbon-carbonyl interactions. The torsion angles of various residues of State I were found to lie in the second and third quadrant of the Ramachandran plot. Consequently, both the carbonyl-carbonyl interactions and formation of hydrogen bonds lack uniformity and regularity. It

is worth mentioning that smaller model oligopeptides of Vim-TBS (58-81) (Table 3) revealed the stability of β-strand structure while in the full length peptide the α-helical structure was observed highlighting the critical relation between peptide length and secondary structure. Consequently, future design paradigms for this peptide need to emphasize and explore this vital relation in order to achieve the best design. This is the first report on the structural characterization of Vim-TBS (58-81) peptide.

3.1.4. *Tat (48-60) peptide*

Two different starting conformations were taken to carry out energy minimization studies viz., State I with starting conformation corresponding to Φ, Ψ values obtained after model oligopeptide minimization and State II with Φ, Ψ values corresponding to the α-helical region (-57°,-47°). State II that adopted a uniform α-helix type secondary structure (Table 4b) except terminal residues, was found to be energetically most stable. Helical secondary structures have already been highlighted in the literature as being necessary for cell penetration properties (*48,49*) because such structures seem essential particularly within the lipid phase of the membrane for its cellular uptake and stabilization. Minimization studies (at a dielectric constant of 4) have revealed that Vim-TBS (58-81) adopts a secondary structure similar to that observed in Tat (48-60), and the same mechanism of cell penetration can be attributed to Vim-TBS (58-81) based on the structure-function and activity relationships (*50,51*).

3.1.5. *p10 peptide*

Similarly, two different starting conformations were selected for energy minimization studies *i.e.*, with α-helix like torsion angles (State I, Table 4b) and with β strand like torsion angles (State II, Table 4b). On the basis of steepest descent and conjugate gradient energy minimization studies, the α-helix secondary structure (State I) was found to be more stable by ~ 62 kcal mol^{-1}.

3.2. *MD simulations*

In general, conformations adopted by proteins/peptides are significantly influenced by local environmental conditions that refer to the solvation interface which communicates bulk properties of the solvent (like temperature, pressure *etc*.) to the peptide and determines localized effects about the proteins/peptides due to specific solute-solvent interactions (*52*). For a better understanding about conformational behavior, dynamic structure, interactions and stability of these peptides in aqueous environment, MD simulation studies were performed in explicit water. Simulation results in terms of Φ, Ψ and ω values for the various

starting conformations of Tat (48-60), Vim-TBS (58-81) and p10 peptides are given in Table 5. Conformation I, II, and III of Vim-TBS (58-81) correspond to the starting geometry with Φ, Ψ, ω values obtained after MM energy minimization studies. Similarly, final conformations obtained after MM studies for Tat (48-60) and p10 peptides were the starting conformations for MD simulation studies.

Simulations in water revealed that all three peptides, Tat (48-60), Vim-TBS (58-81) and p10, adopt either a helical structure or a random conformation in water (Table 5). The energy difference between these two states is ~ 5-6 kcal/mol and is not such that it allows/favors exclusive population of any state especially when one considers the energy contribution of a single hydrogen bond *i.e.* ~ 2-5 kcal/mol (*53,54*). In Vim-TBS (58-81), Conformation II with average Φ, Ψ values of ~ -63°, -54° was energetically more stable with respect to conformation I and III by 6.2 and 11.5 kcal/mol respectively. On the other hand such a helical structure (Conformation II) was energetically less stable by 5 kcal/mol in Tat (48-60) peptide. The stability of these two states is governed by the dominance or contribution of polar contacts between the solvent water molecules and the various backbone and side chain functionalities (intermolecular interactions) of the peptide. Because these two conformations are labile on the energy scale it is argued that in water both helical and random coil like structures co-exist in a dynamic state and moreover, this energy gap can be compensated by the choice of the solvent *i.e.*, in protic or aprotic environment (*55*). It is worth mentioning here that these results are consistent with the NMR and CD spectroscopy results that have shown the occurrence of no regular geometry in Tat (48-60) peptide. Solid-state NMR shows that Tat (48-60) is highly dynamic and adopts a random coil conformation (*56*). The CD spectrum studies of Tat peptide (residues 34-56) have also reported a disordered conformation in buffer solution with a strong negative band at 198 nm and weak positive ellipticity between 212 and 222 nm (*57*). The ^{1}H/^{15}N HSQC spectrum of Tat has also suggested that the protein is undergoing conformational exchange on the millisecond to microsecond time scale, indicating a transient structure formation (*58*). It is also worth mentioning here that almost 30% of the eukaryotic proteome is intrinsically distorted under physiological conditions *i.e.*, in the absence of binding parameters these proteins or protein segments do not fold into a stable conformation but exist in a more or less restricted ensemble of conformations determined by the amino acid sequence (*57*). Utility of this observation lies in the fact that the unfolded proteins have an advantage over folded proteins in providing a much larger surface area enabling multiple interactions with other molecules (*59*).

p10 peptide adopted the helical conformation in its most stable state (Table 5) and was found to be more stable by 5.8 kcal/mol than Conformation II.

Table 5. MD results under NVT conditions for different conformations of Tat (48-60), Vim-TBS (58-81) and p10 peptide after 1 ns simulations with Φ, Ψ, ω values

Vim			p10		Tat	
I	II	III	I	II	I	II
-,-143.8	-,148.6	-,-131.6	-,172	-,135.6	-,121.1	-,-133.5
-	-	-	-	-	-	-
118.1,127.8	-66.4,-161.7	-75.8,-80.3	-54,88.6	-54.4,113.2	-53.5,-41.5	-52.1,-51.7
175.5	-178.1	-175	175.6	167.8	180	-166.8
-42.4,-56	-53.1,-50	-62.9,-49.2	-66,-27	-93,84	-65.5,-44.1	-51,-49.1
-165.8	-179	178	-173.7	-170	-173	180
-90,-22.2	-63.5,-52.3	-98.4,118	-52.8,-65.2	-76.9,80	-74.1,107.5	-65.2,-26.3
-174	-176	170	-177.4	163.4	-173	166.6
-57.2,-51.8	-50,-55	-110.5,130.9	-44.6,-55.4	-94.2,86.2	-65.6,147.6	-63.7,-38.6
179	178	179	165.9	-176	162.2	167.2
-129.4,132	-50.1,-32	-63.2,133.2	-74,-33.4	-76.9,-58	-51.6,-73.7	-67.2,-50
-177	178.2	164.4	-172.1	174.6	166	177.7
59,2.3	-80.2,-57	-124.2,129	-62.7,-52.1	-97.8,123.4	-93.5,-73.6	-57.6,-53.3
-178.6	167.6	175	170.3	-163.3	-166.5	-177.6
57.6,120	-58.6,-54	-167.9,148	-49.3,-34.4	-131,144	-107.2,180	-60.4,-37.7
172.9	-176	-172	164.8	172.3	-178.7	174.2
-155.7,156	-56.1,-50.6	-92,133	-61.7,-47.7	-67,-26.8	13.8,100	-75.2,-27.6
178.3	-176.4	-176	169.2	176.3	-179.2	180
-105,122	-45.3,-52.5	-91,68.2	-58,-38.3	-84.4,-79.1	-119,118.7	-52.6,-44
-171.6	172.4	-178	171.7	-172.5	-165.7	177.3
57.7,145	-85,-29.2	-65,121	-65.6,-51.4	-67.7,119.1	-63.5,150.4	-61.4,-54.9
173	-169	-172.4	178.3	167.7	164.3	168.6
-48.4,-42.6	-70.2,-54	-123.8,83.1	-60.9,-40.7	-108,158.8	-60.3,143.6	-94.6,59.1
-166.8	175.3	176	174	-178.3	171	165.4
-63,-37.8	-53,-52.2	-111.4,103.8	-55.3,-38.6	-135.5,104.1	-140.7,-	-121.8,-
180	172.6	163	172	180	-173.8	171
-104.8,29.2	-45.8,-45	-148.3,157.7	-70,-44	-83.6,127		
178.1	172.6	168	173.3	163.5		
-112,108	-52.4,-35.2	-9.3,-81.3	-65.4,-28.3	-95.6,-162		
170	170.4	178	180	180		
-56,75	-116.5,-32.4	-124,104.9	-76,-52.1	-78.3,142		
-176	-173	-165.4	167	163.4		
-129,120	-55.3,-53.6	36.4,68.7	-112,83.5	-66.8,113.7		
-176	180	173.7	-172.6	160.4		
-63.4,132.6	-50,-51.8	-75.1,139.3	-87.4,-	-126,-		
-173.4	-178.1	177.5	-173.5	-174.8		
-123,-171	-55.4,-61	-97,-107.2				
2.3	179	-167.2				
50,61	-62.1,-27.6	-97.4,-39.3				
177.2	-171	172.5				
-116.7,141	-77,-49	-95.7,148				
169	168	165				
-54.4,-46	-67.7,-38.5	-71.7,104.6				
-177	178.5	180				
-110.8,67.7	-69.3,-91.2	-90,124.6				
172	176	-177				
-142.6,-	-105.9,-	-127.2,-				
177	-168.4	-176.8				
ΔE 6.2	0.0	11.5	0.0	5.8	0.0	5.0

Polar contacts with water which are present in both conformations, the extensive hydrogen network of carbonyl-oxygen of ith residue with the amide hydrogen of the ith+4 residue, ($d_{CO_i...HN_{i+40}} \sim 2.0, 1.8$ Å) along with the strong carbonyl-carbonyl interactions are the major factor in the stability of the helical state.

3.3. *Simulation studies of the fusion peptides*

To establish and analyze the conformational preference of Vim-TBS (58-81) peptide in conjunction with cargo molecules, simulations of the fusion peptide Vim-TBS (58-81)-p10 and Tat (48-60)-p10 were carried out for 1 ns in water under NVT conditions.
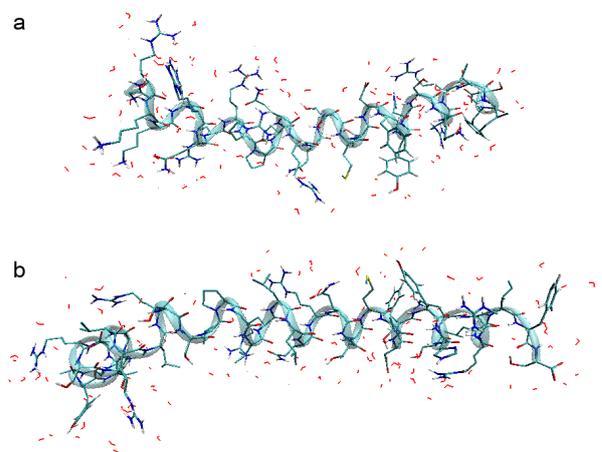
3.3.1. *Tat (48-60)-p10 peptide*

Two different starting conformations were selected for the structural study of the designed fusion peptide Tat (48-60)-p10, with Φ, Ψ values corresponding to those

Table 6. Simulation results for Fusion peptides (Vim-TBS(58-81)-p10 peptide and Tat(48-60)-p10 peptide) after 1ns under NVT conditions

Vim-TBS-p10		Tat-p10	
I	II	I	II
-,-122	-,114.2	-,170	-,161.2
-	-	-	-
80.2,121.4	-76,-166.9	-56.3,-74.1	-51.4,-40
-174	179.5	178.8	-178
-61.6,-26	-67.7,-61.7	-31.6,-51.2	-127.7,-61.4
180	-158.4	171.2	178.1
-75.6,-61.5	-49.8,-55.6	-62.6,-55.6	-38.4,109.1
170	-179	177.6	166.4
-40.2,-52.7	-51.8,-41.1	-44.4,-30.9	-67,165
178	169.8	164.7	-176.6
-78.5,-38	-66,-47.7	-67.5,-56	-63.3,-56.4
-174.3	174.5	165.5	179.4
-96.8,-78.7	-65.1,-46.2	-45.7,-47.8	-125.4,-58.4
178.5	-175.7	173.8	-166.7
-51.7,-52.6	-42.6,-55.8	-52.8,-50.5	-113.8,145.5
-172.3	177.3	174	170.9
-60.3,-56	-65.1,-28.9	-87.7,0.5	68.3,63.5
179.3	-177.3	176.4	173.9
-53.7,-44.8	-71.4,-41.4	-76.5,-40.2	-85.4,111.6
174.6	175.1	-170.6	-176.8
-52.6,-67	-46.5,-43.8	-61.7,-52.4	-73,115.2
175.6	163.5	161.8	175.6
-39.4,-63.3	-78.6,-55	-49,-41.5	-58.6,148.3
174.2	-176.7	175.3	178.6
-48.3,-51.1	-45,-53.7	-54.6,-40.9	-119.4,169.2
171.1	171.4	173.3	-164.4
-38.3,-40	-57.8,-44.3	-71.6,-48.3	-122.2,114.4
177.6	-179	175.3	177.3
-81.7,-30.8	-67.2,-32.5	-61.5,-32.7	70,94.1
166	178.6	-177.7	169.2
-90,-37	-67.5,-40	-71.8,-48.5	-55.4,-52.1
-166.6	175.7	168.6	-173.6
-52,-39.2	-60,-47	-55,-53.4	-43.7,-50
167.6	-171.7	167.4	174
-54.7,-64.3	-57.4,-40	-54.7,-3.2	-69.5,-29
174.1	167.8	-179.1	-175.2
-54.4,-42.8	-65.7,-56.4	-57.8,-54.7	-112,-95
-173.2	-177.7	-176.4	-175.5
-61,-54.3	-59.1,-35	-42.3,-42.4	-35,-66.5
177.5	176	173	176.9
-62.3,-51.5	-75,-28.7	-58,-65.4	-59.2,-51.7
-176.7	-173.9	177.1	180
-50,-44.1	-75,-40.3	-52.3,-41.7	-50.5,-41.9
170.2	175.8	173.8	172.5
-59,-65.3	-70.2,-43.9	-64.7,-39.4	-70,-37.2
171.7	172.8	173	176.4
-46.2,-48	-109.5,91.4	-54.5,-50.1	-48.9,-53.5
-172.4	175	175.3	162.1
-62.5,-44.7	-74.7,147.7	-57.2,-42.1	-57.1,-42.1
180	-164.3	177.4	165.4
-56.2,-38.1	56.6,129.1	-61.4,-53.5	-66.5,-61.8
173.1	-177.8	171.4	173.8
-76.6,-28.7	-77.3,-10	-58.4,-34.4	-53,-25.6
178.8	-174.4	-175.1	-178.5
-81.4,-29	-87,-45.8	-65.7,-45.5	-91,-48.2
166.2	168.8	176.2	178
-63,-48.5	-45.2,-55	-93.1,-21.5	-109.6,-67.4
167.8	171.7	-176.3	-171.5
-59.3,-35.3	-60.4,-40	-128.4,123.3	-116,101.5
173.8	172.5	-172.2	-175
-70.4,-38.1	-60,-45	-75,-	-130.7,-
174.7	-178	-172.5	180
-57.4,-56.6	-61.4,-50.4		
168.5	174.5		
-49.4,-53	-49.2,-55.6		
170.6	169.4		
-58,-56	-56.6,-42.7		
177.3	-179.8		
-54.8,-47.5	-54.1,-55.3		
176	1763.9		
-63.2,-44.6	-51.2,-52		
170.7	167.4		
-70.1,-25.4	-64,-26		
177.3	-176.1		
-70,-27.8	-81.1,-34.8		
162.8	173		
-75.3,-41.7	-60,-48.2		
168.1	171.6		
-65.8,-44.2	-74.6,-22.2		
173	173		
-134.6,136.5	62,67.5		
-176.4	-179		
-142.2,-	-133.5,-		
179	179.3		
ΔE 0.0	16.8	0.0	11.3

Figure 3. Graphical views of the (a) Tat (48-60)-p10 fusion peptide, (b) Vim-TBS (58-81)-p10 fusion peptide; in the most stable α-helical conformations (water molecules within 3 Å of the peptide surface are shown).

obtained after MD simulations of individual peptides (Conformation I) and with Φ, Ψ values of -57°, -47° (Conformation II). In the energetically most stable state it was found to adopt Φ, Ψ values that lie in the α-helical region (Table 6, Figure 3a). Although, Tat peptide is unstructured in solution there are several reports suggesting the possibility of a conformational change to augment binding (*60,61*). These results are also supported by NMR spectroscopy and CD spectroscopy studies of a fusion protein consisting of the activation domain for the unreleased equine infectious anemia
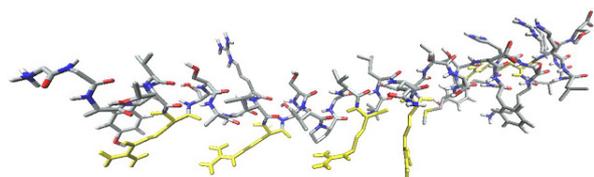
Figure 4. Molecular view of the characteristic amphipathic structure formed in the fusion peptide Vim-TBS (58-81)-p10. The hydrophilic face formed by arginine sidechains is displayed in yellow.

virus and Tat (48-57) that reported a highly helical conformation (*62*). Also 15N NMR relaxation measurements showed that Tat (47-58) became more ordered when binding heparin (*63*). Tat (48-60) has been reported to retain the penetrating properties of the full length HIV-Tat protein (*64*) and also is an effective vehicle for the delivery of biologically active peptide cargoes (*65*). Further, it retains a nuclear localization signal, has relatively low intrinsic toxicity and was thus considered to be an ideal candidate to deliver the p10 peptide to the nucleus. Arginine rich HIV-Tat peptide is able to translocate by destabilizing and inducing transient pores in phospholipid bilayers. The Arginine clusters can strongly interact with lipid head groups on the distal surface of the bilayer to drive translocation. The unstructured CPPs stabilize their backbone polar groups by forming transient intermolecular H-bonds with the lipid phosphates and water (*66*).

3.3.2. *Vim-TBS (58-81)-p10 peptide*

For the complete structural study of Vim-TBS (58-81)-p10 designed fusion peptide, different starting geometries were taken with Φ, Ψ values corresponding to those obtained after MD simulations of individual peptides (Conformation I) and with Φ, Ψ values of -57°, -47° (Conformation II). Simulation results given in Table 6 reveal that the energetically most stable conformation (by 16.8 kcal/mol) corresponds to α-helix type secondary structure with average Φ, Ψ values of -60°, -40°. A molecular representation of this conformational state is shown in Figure 3b. It is evident that although both the fusion peptides form a helical structure in the most stable states but the structure obtained in the case of Vim-TBS-p10 fusion peptide is better characterized in terms of its amphipathic nature with defined hydrophilic and hydrophobic faces as revealed in the molecular view given in Figure 4. A similar structure was reported for Tat-p10 fusion peptide (*67*) and on this basis, it is suggested that the hydrophilic face formed by the positively charged arginine and lysine residues shall thus facilitate a better interaction of this fusion peptide with the membrane. Therefore, we predict Vim-TBS to display better cell penetrating properties and act as a potential drug delivery agent. This finding is well supported by the observations of Balzeau et al. that this fusion peptide

accumulates and distributes in glioblastoma cells (*25*). Furthermore, this fusion peptide crosses the plasma membrane and localizes to the nucleus where p10 maintains its pro-apoptogenic activity. In contrast, when the p10 peptide is ligated to the Tat (48-60) peptide, entry to the nucleus is strongly reduced and its pro-apoptogenic activity is also attenuated (*25*).

4. Discussion

The critical relation between peptide length and secondary structure was highlighted by the formation of stable β-strand like secondary structures in model oligopeptides of Vim-TBS (58-81) while the full length peptide was found to be stable when adopting an α-helical structure. Such structures are particularly stabilized by minimization of steric constraints imposed by the lengthy and/or bulky aromatic and/or charged side chains. In the model oligopeptides of the Tat (48-60) peptide the population of variable conformations contrary to the prediction results further signified the importance of length and nature of the amino acid residues. Also, the type of positively charged residues (lys or arg) played a crucial role in the formation of stable helical secondary structures in short length cationic oligopeptides. Molecular mechanics energy minimization results of the full length peptides, Vim-TBS (58-81), Tat (48-60) and p10, revealed that the energetically most stable conformation formed a characteristic α-helix like secondary structure. In water the three peptides adopted either a helical structure or a random conformation with an energy difference between the two states being ~ 5-6 kcal/mol which is not large enough to allow exclusive population of any state. The peptide Vim-TBS (58-81) had average Φ, Ψ values of ~ -63°, -54° while in the Tat (48-60) peptide such a helical structure was marginally less stable. The stability of either of the two states is administered by the formation of polar contacts between the solvent water molecules and the various backbone and side chain functionalities (intermolecular interactions) of the peptide. Because these two conformations are labile on the energy scale it is argued that in water both helical and random coil like structures co-exist in a dynamic state. To establish and analyze the conformational preference of Vim-TBS (58-81) peptide in conjunction with cargo molecules, simulations of the fusion peptide Vim-TBS (58-81)-p10 and Tat (48-60)-p10 were carried out. Although, both fusion peptides formed helical structures the structure obtained for the fusion peptide; Vim-TBS-p10 is relatively better characterized in terms of its amphipathic nature with defined hydrophilic and hydrophobic faces. Consequently, the hydrophilic face formed by the positively charged residues should facilitate a better interaction of this fusion peptide with the membrane as compare to that of the Tat-p10 peptide. Such an acquired amphipathicity upon secondary structure induction

may guide the anchoring of the CPP in the hydrophobic region of the membrane. Thus, we predict Vim-TBS (48-60) peptide to display better cell penetrating properties and hence, act as a potential drug delivery agent.

References

1. Lindgren M, Hallbrink M, Prochiantz A, Langel U. Cell-penetrating peptides. Trends Pharmacol Sci. 2000; 21:99-103.
2. Fatemeh M, Lindberg S, Langel U, Futaki S, Graslund A. Mechanisms of cellular uptake of cell-penetrating peptides. J Biophys. 2011; 2011:1-10.
3. Trabulo S, Resina S, Simoes S, Lebleu B, Lima PMC. A non-covalent strategy combining cationic lipids and CPPs to enhance the delivery of splice correcting oligonucleotides. Mol Ther Nucleic Acids. 2010; 145:149-158.
4. Brooks NA, Pouniotis DS, Tang CK, Apostolopoulos V, Pietersz GA. Cell-penetrating peptides: Application in vaccine delivery. Biochim Biophys Acta. 2010; 1805:25-34.
5. Endoh T, Ohtsuki T. Cellular siRNA delivery using cell-penetrating peptides modified for endosomal escape. Adv Drug Deliv Rev. 2009; 61:704-709.
6. Foged C, HM Nielsen. Cell-penetrating peptides for drug delivery across membrane barriers. Expert Opin Drug Deliv. 2008; 5:105-117.
7. Grdisa M. The delivery of biologically active (therapeutic) peptides and proteins into cells. Curr Med Chem. 2011; 18:1373-1379.
8. Jafari M, Chen P. Peptide mediated siRNA delivery. Curr Top Med Chem. 2009; 9:1088-1097.
9. Johnson RM, Harrison SD, Maclean D. Therapeutic applications of cell-penetrating peptides. Methods Mol Biol. 2011; 683:535-551.
10. Stewart KM, Horton KL, Kelley SO. Cell-penetrating peptides as delivery vehicles for biology and medicine. Org Biomol Chem. 2008; 6:2242-2255.
11. Torchilin VP. Cell penetrating peptide-modified pharmaceutical nanocarriers for intracellular drug and gene delivery. Biopolymers 2008; 90:604-610.
12. Snyder EL, Dowdy SF. Cell penetrating peptides in drug delivery. Pharmaceutical Research. 2004; 21:3.
13. Niesner U, Halin C, Lozzi L, Gunthert M, Neri P, Wundern-Allenspach H, Zardi L, Neri D. Quantitation of the tumor-targeting properties of antibody fragments conjugated to cell-permeating HIV-1 TAT peptides. Bioconjug Chem. 2002; 13:729-736.
14. Astriab-Fisher A, Sergueev D, Fisher M, Shaw BR, Juliano RL. Conjugates of antisense oligonulceosides with the Tat and antenapedia cell-penetrating peptides: Effects on cellular uptake, binding to target sequences, and biologic actions. Pharm Res. 2002; 19:744-754.
15. Torchilin VP, Levchenko TS, Rammohan R, Volodina N, Papahadjopoulos-Stenberg B, D'Souza GC. Cell transfection *in vitro* and *in vivo* with nontoxic TAT peptide–liposome–DNA complexes. Proc Natl Acad Sci USA. 2003; 100:1972-1977.
16. Herce, HD, Garcia AE. Molecular dynamics simulations suggest a mechanism for translocation of the HIV-1 TAT peptide across lipid membranes. Proc Natl Acad Sci USA. 2007; 104:20805-20810.
17. Kersemans V, Kersemans K, Comelissen B. Cell penetrating peptides for *in vivo* molecular imaging applications. Curr Pharm Des. 2008; 14:2415-2447.
18. Zorko M, Langel U. Cell-penetrating peptides: Mechanism and kinetics of cargo delivery. Adv Drug Del Reviews. 2005; 57:529-545.
19. Eiríksdóttir E, Konate K, Langel U, Divita G, Deshayes S. Secondary structure of cell-penetrating peptides controls membrane interaction and insertion. Biochim Biophys Acta. 2010; 1798:1119-1128.
20. Morris MC, Depollier J, Mery J, Heitz F, Divita G. A peptide carrier for the delivery of biologically active proteins into mammalian cells. Nat Biotechnol. 2001; 19:1173-1176.
21. Meade BR, Dowdy SF. Exogenous siRNA delivery using peptide transduction domains/cell penetrating peptides. Adv Drug Deliv Rev. 2007; 59:134-140.
22. Coulombe PA, Wong P. Cytoplasmic intermediate filaments revealed as dynamic and multipurpose scaffolds. Nature Cell Biol. 2004; 6:699-706.
23. Raphael B, Julien B, Peterson AC, Eyer J. The vimentin-tubulin binding site peptide (Vim-TBS.58-81) crosses the plasma membrane and enters the nuclei of human glioma cells. Int J Pharma. 2011; 423:77-83.
24. Richard JP, Melikov K, Vives E, Ramos C, Verbuere B, Gait MJ, Chernomordik LV, Lebleu B. Cell-penetrating peptides. A reevaluation of the mechanism of cellular uptake. J Biol Chem. 2003; 278:585-590.
25. Balzeau J, Peterson A, Eyer J. The vimentin-tubulin binding site peptide (Vim-TBS.58-81) crosses the plasma membrane and enters the nuclei of human glioma cells. Int J Pharm. 2012; 4:77-83.
26. Baker RD, Howl J, Nicholl ID. A sychnological cell penetrating peptide mimic of p21 (WAF1/CIP1) is pro-apoptogenic. Peptides 2007; 28:731-740.
27. Mutoh M, Lung FD, Long YQ, Roller PP, Sikorski RS, Connor PMO. A p21(Waf1/Cip1) carboxyl-terminal peptide exhibited cyclin-dependent kinase-inhibitory activity and cytotoxicity when introduced into human cells. Cancer Res. 1999; 59:3480-3488.
28. Warbrick E, Lane DP, Glover DM, Cox LS. A small peptide inhibitor of DNA-replication defines the site of interaction between the cyclin-dependant kinase inhibitor p21(WAF1) and proliferating cell nuclear antigen. Curr Biol. 1995; 5:275-282.
29. Jones AT. Protein secondary structure prediction based on position-specific scoring matrices. J Mol Biol. 1999; 292:195-202.
30. Johansson MU, Zoete V, Michielin O, Guex N. Defining and searching for structural motifs using DeepView/Swiss-PdbViewer. BMC Bioinformatics. 2012; 13:173.
31. Van der Spoel D, Lindahl E, Hess B, van Buuren AR, Apol E, Meulenhoff PJ, Tieleman DP, Sijbers ALTM, Feenstra KA, Van Drunen R, Berendsen HJC. Gromacs User Manual version 3.3, 2005.
32. Berendsen HJC, Postma JPM, Van Gunsteren WF, Hermans J. Intermolecular Forces: Interaction models for water in relation to protein hydration. D. Reidel Publishing Company, Dordrecht, 1981; 331-342.
33. Hockney RW, Eastwood JW. Computer simulation using particles. McGraw-Hill, New York, USA, 1981.
34. Berendsen HJC, Postma JPM, DiNola A, Haak JR. Molecular dynamics with coupling to an external bath. J Chem Phys. 1984; 81:3684-3690.
35. Hess B, Bekker H, Berendsen HJC, Fraaije JGEM. A linear constraint solver for molecular simulations. J

Comp Chem. 1997; 18:1463-1472.

36. Essmann U, Perera L, Berkowitz ML, Darden T, Lee H, Pedersen LG. A smooth particle mesh Ewald method. J Chem Phys. 1995; 103:8577-8592.

37. Humphrey W, Dalke A, Schulten K. VMD-Visual Molecular Dynamics. J Molec Graphics. 1996; 14:33-38.

38. Nandel FS, Saini A. Peptoids with aliphatic sidechains as helical structures without hydrogen bonds and collagen/inverse-collagen type structures. Journal of Biophysical Chemistry 2011; 2:37-48.

39. Nandel FS, Saini A. Construction and design of single stranded collagen-like structure. Indian journal of biochemistry & biophysics. 2007; 44:106-113.

40. Nandel FS, Saini A. Conformational study of short peptoid models for future applications as potent antimicrobial compounds. Macromolecular Theory and Simulations. 2007; 16:295-303.

41. Alias M, Ayuso-Tejedor S, Fernandez-Recio J, Cativiela C, Sancho J. Helix propensities of conformationally restricted amino acids. Non-natural substitutes for helix breaking proline and helix forming alanine. Org Biomol Chem. 2010; 8:788-792.

42. Voet D, Voet JG, Pratt CW. Fundamentals of Biochemistry. John Wiley and Sons, New York, 2004.

43. Gunasekaran K, Nagarajaram HA, Ramakrishnan C, Balaram P. Stereochemical Punctuation Marks in Protein Structures: Glycine and Proline Containing Helix Stop Signals. J Mol Biol. 1998; 275:917-932.

44. Nandel FS, Jaswal R. New Type of Helix and 2_7 Ribbon Structure Formation in Poly ΔLeu Peptides: Construction of a Single-Handed Template. Biomacromolecules. 2007; 8:3093-3101.

45. Niidome T, Takaji K, Urakawa M, Ohmori N, Wada A, Hirayama T, Aoyagi H. Chain length of cationic α-helical peptide sufficient for gene delivery into cells. Bioconjugate chemistry. 1999; 10:773-780.

46. Hilda C, Arellano A. Secondary structure prediction of protamines. Int J Biol Macromol. 1982; 1:3-8.

47. Aduzbei AA, Sternberg JE. Left-handed polyproline II helices commonly occur in globular proteins. J Mol Biol. 1993; 229:472-493.

48. Vives E, Brodin P, Lebleu B. A truncated HIV-1 Tat protein basic domain rapidly translocates through the plasma membrane and accumulates in the cell nucleus. J Biol Chem. 1997; 272:16010-16017.

49. Mujeeb A, Bishop K, Peterlin BM, Turck C, Parslow TG, James TL. NMR structure of a biologically active peptide containing the RNA-binding domain of human immunodeficiency virus type 1 Tat. Proc Natl Acad Sci U S A. 1994; 91:8248-8252.

50. Ambriz-Rivas M, Pastor N, Rio GD. Relating Protein Structure and Function Through a Bijection and Its Implications on Protein Structure Prediction. Protein Interactions. Dr. Jianfeng Cai (Ed.), 2012; ISBN: 978-953-51-0244-1.

51. Mirsky AE, Pauling L. On the structure of native, denatured, and coagulated proteins. Proc Natl Acad Sci U S A. 1936; 22:439-447.

52. Nemethy G, Peer WJ, Scheraga HA. Effect of Protein-Solvent Interactions on Protein Conformation Annual Review of Biophysics and Bioengineering 1981; 10: 459-497.

53. Mitchell JBO, Price SL. The nature of the N-H O=C hydrogen bond-- An intermolecular perturbation-theory study of the formamide formaldehyde complex. J Comp Chem. 1990; 11: 1217-1233.

54. BenTal N, Sitkoff D, Topol IA, Yang AS, Burt SK, Honig B. Free energy of amide hydrogen bond formation in vacuum, in water, and in liquid alkane solution. J Phys Chem B 1997; 101: 450-457.

55. Miranda LP, Alewood PF. Chemistry-Accelerated chemical synthesis of peptides and small proteins. Proc Natl Acad Sci USA 1999; 96: 1181-1186.

56. Yongchao S, Alan JW, Ruchala P, Hong M. Membrane-bound dynamic structure of an arginine-rich cell-penetrating peptide, the protein transduction domain of HIV Tat, from solid-state NMR. Biochemistry 2010; 49:6009-6020.

57. McQueen P, Donald LJ, Vo TN, Nguyen DH, Griffiths H, Shojania S, Standing KG, O'Neil JD. Tat peptide-calmodulin binding studies and bioinformatics of HIV-1 protein–calmodulin interactions. Proteins. 2011; 79:2233-2246.

58. Shojania S, O'Neil JD. HIV-1 Tat is a natively unfolded protein: the solution conformation and dynamics of reduced HIV-1 Tat-(1-72) by NMR spectroscopy. J Biol Chem. 2006; 281:8347-8356.

59. Gunasekaran K, Tsai CJ, Kumar S, Zanuy D, Nussinov R. Extended disordered proteins: targeting function with less scaffold. Trends Biochem Sci. 2003; 28:81-85.

60. Dennison SR, Baker RD, Nicholl ID, Phoenix DAInteractions of cell penetrating peptide Tat with model membranes: A biophysical study. Biochemical and Biophysical Research Communications. 2007; 363:178-182.

61. Tunnemann G, Martin RM, Haupt S, Patsch C, Edenhofer F, Cardoso MC. Cargo-dependent mode of uptake and bioavailability of TAT-containing proteins and peptides in living cells. FASEB J. 2006; 20:1775-1784.

62. Puglisi JD, Tan R, Calnan BJ, Frankel AD, Williamson JR. Conformation of the TAR RNA–arginine complex by NMR spectroscopy. Science. 1992; 257:76-80.

63. Hakansson S, Caffrey M. Structural and dynamic properties of the HIV-1 tat transduction domain in the free and heparin-bound states. Biochemistry. 2003; 42:8999-9006.

64. Thoren PE, Persson D, Lincoln P, Norden B. Membrane destabilizing properties of cell-penetrating peptides. Biophys Chem. 2005; 114:169-179.

65. Kaplan IM, Wadia JS, Dowdy SF. Cationic TAT peptide transduction domain enters cells by macropinocytosis. J Control Release. 2005; 102:247-253.

66. Su Y, Waring AJ, Ruchala P, Hong M. Membrane-bound dynamic structure of an arginine-rich cell-penetrating peptide, the protein transduction domain of HIV–Tat from solid-state NMR. Biochemistry. 2010; 49:6009-6020.

67. Ho A, Schwarze SR, Mermelstein SJ, Waksman G, Dowdy SF. Synthetic Protein Transduction Domains: Enhanced Transduction Potential *in vitro* and *in vivo*. Cancer Res. 2001; 61:474-477.